

# Heavy-fermion metallic state and Mott transition induced by Li-ion intercalation in $\text{LiV}_2\text{O}_4$ epitaxial films

Tatsuya Yajima <sup>1,\*</sup> Takuto Soma <sup>1</sup> Kohei Yoshimatsu <sup>1</sup> Nobuyuki Kurita <sup>2</sup>  
Masari Watanabe <sup>2</sup> and Akira Ohtomo <sup>1,3,†</sup>

<sup>1</sup>*Department of Chemical Science and Engineering, Tokyo Institute of Technology, 2-12-1 Ookayama, Meguro-ku, Tokyo 152–8552, Japan*

<sup>2</sup>*Department of Physics, Tokyo Institute of Technology, 2-12-1 Ookayama, Meguro-ku, Tokyo 152–8551, Japan*

<sup>3</sup>*Materials Research Center for Element Strategy (MCES), Tokyo Institute of Technology, Yokohama 226–8503, Japan*



(Received 4 December 2020; revised 16 September 2021; accepted 15 November 2021; published 2 December 2021)

The spinel-type  $\text{LiV}_2\text{O}_4$  exhibits heavy-fermion metallic behaviors at low temperatures, but the effect of composition modulation on them is unknown. We realized the epitaxial growth of highly crystalline  $\text{LiV}_2\text{O}_4$  films and conducted the electrochemical Li-ion intercalation (electron doping) to investigate systematic variation of transport properties in  $\text{Li}_{1+x}\text{V}_2\text{O}_4$ . We found that adjustment of Li content during pulsed-laser deposition was important to obtain films exhibiting the heavy-fermion metallic behavior comparable to that of a bulk single crystal. At low doping regime ( $x \leq 0.5$ ), resistivity increased with increasing electron filling. The slope of their linear  $T^2$  dependence also increased in accordance of a Fermi-liquid model. At high doping regime ( $x > 0.5$ ), a Mott transition was observed over a range of Li content where a new spinel phase and the original one coexisted. The results revealed that the electron doping induced enhancement of the electron correlation and the resultant Mott transition.

DOI: [10.1103/PhysRevB.104.245104](https://doi.org/10.1103/PhysRevB.104.245104)

## I. INTRODUCTION

A class of strongly correlated metals exhibiting large enhancement of the effective mass of carriers below certain temperatures is called heavy-fermion (HF) systems. The HF behaviors are mostly observed in  $f$ -electron intermetallic compounds, while they are rarely observed in  $d$ -electron compounds [1]. A spinel-type  $\text{LiV}_2\text{O}_4$  is the first discovered  $d$ -electron HF system [2], and its properties have been enthusiastically studied by means of transport, specific heat, magnetization, optical measurements, and theoretical calculations [3–13]. The stoichiometric single crystals of  $\text{LiV}_2\text{O}_4$  exhibiting metallic conductivity down to low temperatures are essential to accessing the heavy-fermionic ground state [6,7,9]. The exceptional HF behaviors of  $\text{LiV}_2\text{O}_4$  are thought to be associated with mixed-valent  $\text{V}^{3.5+}$  and/or geometrical spin frustration in the triangular lattice [4,6,10], but no significant evidence has been found yet. To clarify the origin, the modulation of HF metallic states by applying magnetic field [9] or pressure [11] was attempted. On the other hand, there has been no study of the chemical doping, although it is one of the most fundamental approaches to access the evolution of electronic phases. The substitutional doping with divalent ions ( $\text{Mg}^{2+}$  and  $\text{Zn}^{2+}$ ) at Li sites is previously studied only for polycrystalline samples [14–16]. In those studies, electron doping leads to systematic increase in the resistivity that is reminiscent of a conventional Mott transition. However, the metallic conductivity is not observed in the entire range of doping, even for pristine  $\text{LiV}_2\text{O}_4$ . Due to insufficient crys-

tallinity, therefore, intrinsic effects of electron doping on HF metallic ground states in  $\text{LiV}_2\text{O}_4$  still remain largely unexplored.

In recent years, electrochemical Li-ion intercalation has been employed as the ideal electron-doping method [17–19]. The reversible redox reactions allow one to induce a large number of carriers without introducing disorder in a host structure. The normal spinel-type  $\text{LiV}_2\text{O}_4$  once attracted attention as an electrode material for the Li-ion secondary battery [20–22]. As  $\text{LiMn}_2\text{O}_4$  can be used for the cathode of a commercial Li-ion secondary battery [23], the spinel-type transition-metal oxides are of advantage for topochemical Li-ion (de)intercalations with keeping their host structures. Therefore, Li-ion electrochemical reaction enables the ideal electron-doping study on  $\text{LiV}_2\text{O}_4$ .

To implement such a setup, a single crystalline sample in the form of a thin film is required. Large surface area and small volume provide an advantage on homogeneous electrochemical doping [17], which is not readily realized on bulk samples [24]. However, the epitaxial growth of  $\text{LiV}_2\text{O}_4$  thin films has not been attained yet partly because of highly volatile nature of Li species [25,26].

In this study, we established epitaxial growth of the (111)-oriented  $\text{LiV}_2\text{O}_4$  thin films which exhibit HF behaviors in their transport properties. In order to investigate transport properties of electron-doped  $\text{Li}_{1+x}\text{V}_2\text{O}_4$  films, we employed electrochemical Li-ion intercalation and measured temperature dependence of resistivity. Electron doping induced systematic increase in a lattice parameter and resistivity and eventually a metal-insulator transition (MIT). At  $x \leq 0.5$ , the HF behaviors, which were well described by a Fermi-liquid model, were maintained. In contrast, we found phase-separation behaviors at  $x > 0.5$ . In addition, the slope

\*Corresponding author: yajima.t.ac@m.titech.ac.jp

†aohtomo@apc.titech.ac.jp

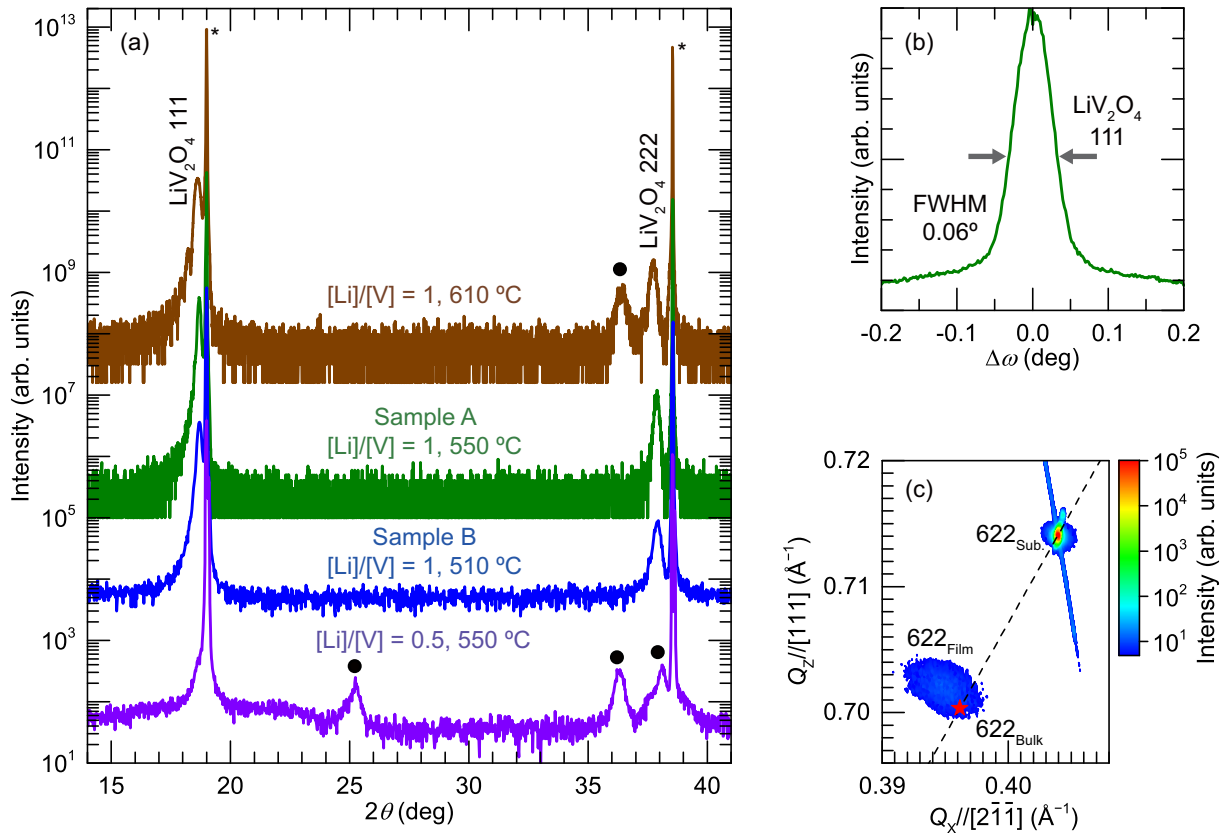


FIG. 1. Structural properties of Li-V-O films. (a) Out-of-plane XRD profiles for films grown at various temperatures by using stoichiometric and Li-rich targets. The asterisks (\*) and closed circles indicate reflections from the  $\text{MgAl}_2\text{O}_4$  (111) substrates and secondary phases, respectively. (b)  $\omega$ -scan rocking curve profile of the  $\text{LiV}_2\text{O}_4$  111 reflection for Sample A. (c) Reciprocal space map for Sample A. The reciprocal point of the  $\text{LiV}_2\text{O}_4$  622 reflection estimated for bulk [7] is indicated by the star. The dashed line intersects the axis origin.

of  $T^2$ -linear resistivity increased in the vicinity of Mott transition and phase separation. Our results demonstrate exceptionally strong electron correlation in  $\text{Li}_{1+x}\text{V}_2\text{O}_4$ . In addition, our approach will pave a way to filling control of Li-containing materials, whose single crystals with various compositions are rarely prepared.

## II. EXPERIMENT

The Li-V-O films were grown on  $\text{MgAl}_2\text{O}_4$  (111) substrates by using pulsed-laser deposition (PLD) equipped with a high-vacuum chamber and KrF excimer laser pulses (10 Hz,  $0.6\text{ J cm}^{-2}$ ). The ceramic tablets used for the laser-ablation targets were prepared by conventional solid-state reactions.  $\text{Li}_2\text{CO}_3$  and  $\text{V}_2\text{O}_3$  (both 3N purity) powders with different compositions ( $[\text{Li}]/[\text{V}] = 0.5, 1.0, \text{ and } 1.5$ ) were mixed, pelletized, and sintered at  $520\text{--}540^\circ\text{C}$  several times until carbonate species decomposed completely. Substrate temperature was set in a range from  $510^\circ\text{C}$  to  $610^\circ\text{C}$ .  $\text{Ar}/\text{H}_2$  gas (1 vol%  $\text{H}_2$ ) was continuously fed into the chamber with keeping the pressure of 0.1 mTorr during the growth. Film thickness ranged from 30 to 100 nm as evaluated by a stylus-type profiler, and 50–70-nm-thick samples were used for transport measurements. The flat surface with a root-mean-square roughness of  $\sim 1.0$  nm was verified by using atomic force microscopy. The structural properties before and after Li-ion electrochemical reactions were investigated by a x-ray

diffraction (XRD) apparatus (SmartLab, Rigaku) with the  $\text{Cu K}\alpha_1$  radiation. The temperature dependence of resistivity was measured by a standard four-probe method using physical property measurement systems (PPMS) equipped with the He-3 option (Quantum Design).

The Li-ion electrochemical reactions were performed with a three-electrode electrochemical cell. The  $\text{LiV}_2\text{O}_4$  films,  $\text{LiCoO}_2/\text{Al}$  foil (AA Portable Power Corporation), and Ag wire (Nilaco, 4N purity) were used for working, counter, and quasireference electrodes, respectively. Electrolyte solution ( $1\text{ mol L}^{-1}$ ) was prepared by mixing  $\text{LiClO}_4$  ( $>99\%$  purity) and propylene carbonate (PC) ( $>98\%$  purity) in a glovebox under Ar atmosphere. The solution was heated at  $\sim 50^\circ\text{C}$  in a vacuum to remove moisture before the electrode was immersed in it. Cyclic voltammetry and chronoamperometry were performed with a potentiostat (AMETEK SI, VersaSTAT4) at room temperature (RT) in air or under a vacuum in the PPMS chamber. The transport properties were obtained by repeating chronoamperometry followed by temperature-dependent resistivity measurements under a vacuum in the PPMS chamber.

## III. RESULTS AND DISCUSSION

Careful adjustment of target compositions and growth conditions was found to be important for accomplishing the epitaxial growth of  $\text{LiV}_2\text{O}_4$  films. Figure 1(a) shows the

out-of-plane XRD profiles for the films grown at various temperatures by using two targets with different compositions. When a stoichiometric target with  $[\text{Li}]/[\text{V}] = 0.5$  was used, only reflections that could not be assigned to the spinel-type  $\text{LiV}_2\text{O}_4$  appeared. The sublimation of Li species often occurs during PLD, giving rise to the formation of Li-deficient phases [25,26]. We verified this tendency and prevented the Li deficiency by using a Li-rich target ( $[\text{Li}]/[\text{V}] = 1.0$ ). In this case, the films showed clear  $hhh$  reflections of the spinel-type  $\text{LiV}_2\text{O}_4$  [7], although a secondary phase appeared when grown at higher temperature (610°C). In the following sentences, the films grown at 550 and 510°C are referred to as Sample A and B, respectively. They indicated the identical peak position and peak width to each other, but their transport properties were substantially different due to the film stoichiometry and antisites, which will be discussed later.

Figure 1(b) shows the  $\omega$ -scan rocking curve profile of the  $\text{LiV}_2\text{O}_4$  111 reflection for Sample A. The full width at half maximum was found to be  $0.06^\circ$ , indicating high crystallinity. To investigate the epitaxial relationships, we took a reciprocal space map around the  $\text{MgAl}_2\text{O}_4$  622 reflection, as shown in Fig. 1(c). The in-plane orientation relationship was verified to be  $\text{LiV}_2\text{O}_4$   $[2\bar{1}\bar{1}] \parallel \text{MgAl}_2\text{O}_4$   $[2\bar{1}\bar{1}]$ . In addition, the position of film spot was almost identical to that estimated from a lattice parameter of bulk ( $a = 8.2437 \text{ \AA}$  [7]). The out-of-plane  $d_{111}$  and in-plane  $d_{2\bar{1}\bar{1}}$  values were calculated to be 4.746 and 3.378  $\text{\AA}$ , which were comparable to bulk values of 4.759 and 3.365  $\text{\AA}$ , respectively. These results strongly supported the stoichiometric composition as well as high crystallinity without any strain from substrates. We note that the use of another target with  $[\text{Li}]/[\text{V}] = 1.5$  resulted in the degradation of crystallinity probably due to excess Li content in the films.

Figure 2 shows the temperature dependence of resistivity  $\rho$  for the  $\text{LiV}_2\text{O}_4$  films and references of bulk single crystal [6] and polycrystal [14]. The transport properties were found to be sensitive to the growth temperature. Despite the identical structural properties, Sample A exhibited metallic behavior ( $d\rho/dT > 0$ ) with a clear drop of  $\rho$  below  $\sim 20$  K, while Sample B exhibited insulating behavior ( $d\rho/dT < 0$ ) below 180 K. Such a deterioration in transport properties is reported even for bulk single crystals [7].

In the previous studies on bulk single crystals, clear metallic behaviors were seen with the drop of  $\rho$  below 20–30 K, which was a sign of HF [6,7,9]. In contrast, bulk polycrystals always kept insulating properties up to RT [14–16]. As for the Sample A,  $\rho$  at 300 and 2 K was 2.1 and 0.53  $\text{m}\Omega \text{ cm}$ , respectively. These values are larger than those of bulk single crystal with the highest quality (0.8 and 0.04  $\text{m}\Omega \text{ cm}$ , respectively [6]) by an order of magnitude. Despite the deviations of  $\rho$ , the observed steep drop is similar to each other. Moreover, Sample A exhibited clear HF behaviors: the  $\rho$ – $T$  curves below 2 K obeyed the Fermi-liquid model, and could be fitted to  $\rho = \rho_0 + AT^2$ , where  $\rho_0$  is residual resistivity and coefficient  $A$  is a characteristic parameter being proportional to square of effective mass of carriers  $m^*$  (inset of Fig. 2). The estimated  $A$  ( $7.5 \mu\Omega \text{ cm K}^{-2}$ ) was comparable to that of bulk single crystal ( $2.0 \mu\Omega \text{ cm K}^{-2}$  [6]). This fact suggests that high-quality epitaxial films also formed HF ground state with large  $m^*$ . The  $A$  larger than that of bulk may be inherent in a thin film form with higher resistivity.

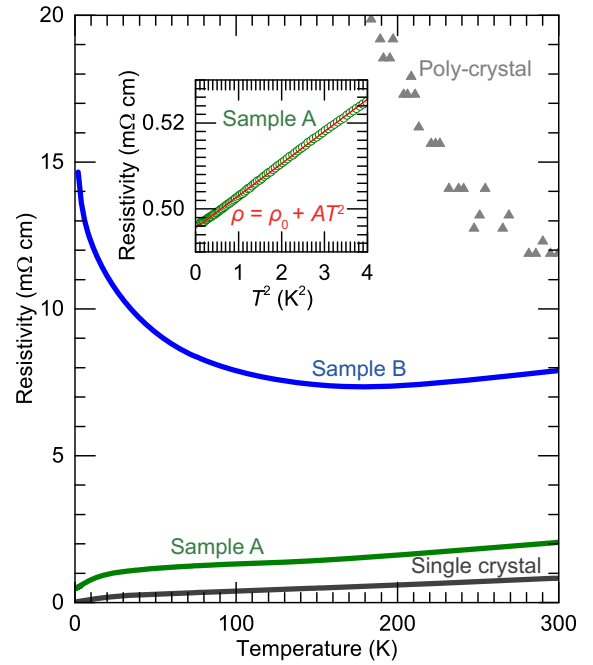


FIG. 2. Temperature dependence of the resistivity ( $\rho$ ) for the  $\text{LiV}_2\text{O}_4$  films (Samples A and B). Data for bulks are also plotted as in Refs. [6,14]. The inset shows the linear  $T^2$  dependence of resistivity for as-grown films below 2 K.

The insulating behavior in Sample B would have been caused by excess Li at antisites derived from nonequilibrium of PLD. For example, in  $\text{Li}_{1+x}\text{Ti}_{2-x}\text{O}_4$  (often written as  $\text{Li}[\text{Li}_x\text{Ti}_{2-x}]\text{O}_4$  with emphasis on site position), excess Li atoms are known to substitute Ti atoms at octahedral sites, which introduce disorder in a Ti-O conduction network to reduce the metallicity [27]. The amount of antisite Li atoms in  $\text{Li}[\text{Li}_x\text{Ti}_{2-x}]\text{O}_4$  can be estimated by degree of the lattice contraction, which arises from reduced average of ionic radii at the octahedral site [28]. We noticed the possibility of antisite  $\text{Li}[\text{Li}_x\text{V}_{2-x}]\text{O}_4$ , which has not been reported, and the difference from the case of  $\text{Li}[\text{Li}_x\text{Ti}_{2-x}]\text{O}_4$ . Taking the ionic radii of  $\text{Li}^+$ ,  $\text{V}^{3+}$ , and  $\text{V}^{4+}$  into account [29], we find an interesting coincidence. The contribution of  $[\text{Li}^+_{\text{V}}]$  on average of the octahedral ionic radii is exactly counterbalanced by the sum of those of deficient  $[\text{V}^{3+}_{\text{V}}]$  and excess  $[\text{V}^{4+}_{\text{V}}]$ , resulting in a constant lattice parameter as long as oxygen stoichiometry is preserved. In detail, given radii of each ion at the octahedral site (76, 64, and 58 pm for  $\text{Li}^+$ ,  $\text{V}^{3+}$ , and  $\text{V}^{4+}$ , respectively), their average in  $\text{Li}[\text{Li}_x\text{V}_{2-x}]\text{O}_4$  will be a constant of 61 pm ( $= [76x + 64(1-3x) + 58(1+2x)]/2$  [pm]). This would be one of the reasons why Samples A and B indicated the identical peak positions despite different  $\rho$ – $T$  curves [Figs. 1(a) and 2]. Note that there is no report of excess Li at the antisite in bulk samples prepared with conventional techniques. This may be a problem inherent in our Li-rich films grown directly by PLD under highly nonequilibrium conditions. Therefore, the possibility of antisite Li should be ruled out in the following results and discussions.

Having established the structural and transport properties comparable to bulk single crystals, we investigated modulation of the transport properties for the  $\text{Li}_{1+x}\text{V}_2\text{O}_4$  films

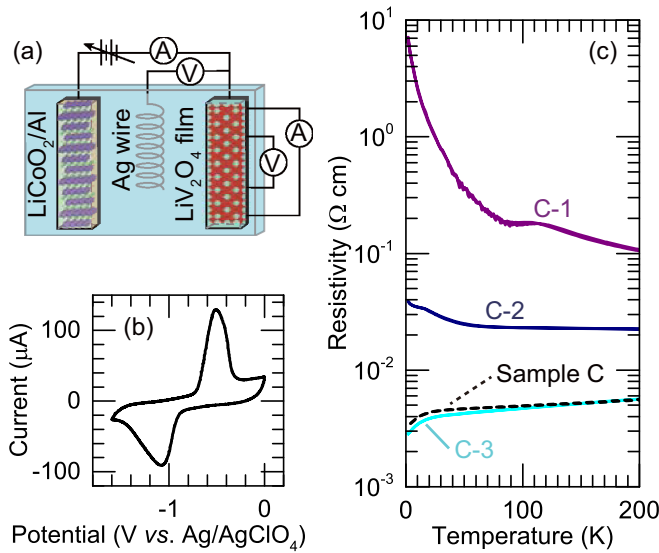


FIG. 3. (a) Schematic illustration of a  $\text{LiV}_2\text{O}_4$   $[\text{LiClO}_4 : \text{PC}]/\text{LiCoO}_2/\text{Al}$  electrochemical cell. (b) Cyclic voltammogram measured at RT by sweeping voltage with 200 mV/s. (c) Temperature dependence of the resistivity for the as-grown  $\text{LiV}_2\text{O}_4$  film (Sample C; dashed line) and Li-ion (de)intercalated  $\text{Li}_{1+x}\text{V}_2\text{O}_4$  films [Samples C-1 ( $-2$  V), C-2 ( $-0.2$  V), and C-3 (0 V); solid lines].

by Li-ion electrochemical reactions. Using a setup shown in Fig. 3(a), *in situ*  $\rho$ - $T$  measurements were performed, which enabled us to study an electronic phase transition in a single sample. Indeed, good cell performance was verified from the cyclic voltammogram [Fig. 3(b)]. Symmetric and sharp redox peaks suggested that the  $\text{LiV}_2\text{O}_4$  film was capable of reversible electrochemical doping through a reaction of  $\text{LiV}_2\text{O}_4 + x\text{Li}^+ + xe^- \rightleftharpoons \text{Li}_{1+x}\text{V}_2\text{O}_4$  [21]. Different from antisite  $\text{Li}[\text{Li}_x\text{V}_{2-x}]\text{O}_4$  discussed above, Li-ion intercalated  $\text{Li}_{1+x}[\text{V}_2]\text{O}_4$  maintains the V-O network [20]. Even in the case of thin films, it would be considered that there is no antisite defect due to Li-ion intercalation. In the following experiment, temperature and cell potential were strictly controlled so that the electrodes were prevented from unintentional incorporation and/or removal of Li ions. First, Li-ion intercalation reaction in the liquid electrolyte was performed at 300 K. Then, the electrochemical cell was cooled to 230 K (a freezing point of  $\text{LiClO}_4:\text{PC}$ ), while applying an open-circuit potential. After completion of freezing, temperature was decreased to 1.9 K and then increased up to 230 K, while measuring  $\rho$  without applying external potential. Finally, the cell was warmed from 230 to 300 K, while applying an open-circuit potential.

The *in situ*  $\rho$ - $T$  curves shown in Fig. 3(c) demonstrates the reversible electrochemical doping for Sample C, which was prepared under the condition same as that of Sample A. After a potential of  $-2$  V was applied,  $\rho$  increased by more than an order of magnitude and the resultant  $\rho$ - $T$  curve indicated insulating behavior (C-1). After the reverse potential of  $-0.2$  V was applied (C-2), however,  $\rho$ - $T$  curve was located near a crossover between metallic and insulating behaviors. In addition, the metallic state with the drop of  $\rho$  below  $\sim 20$  K was perfectly recovered by applying subsequent potential of 0 V

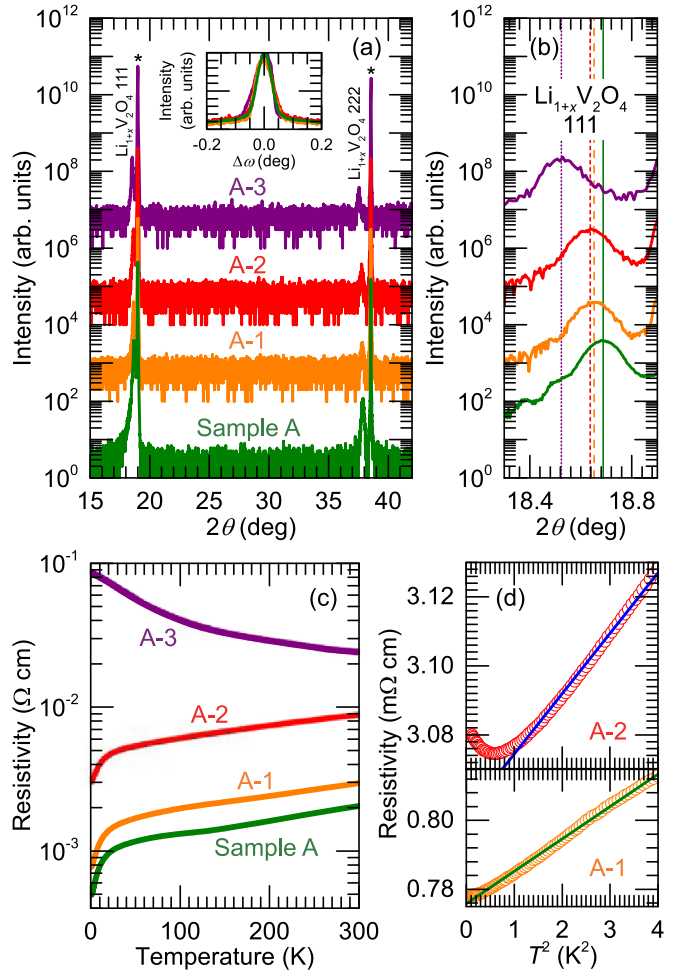


FIG. 4. Electrochemically modulated properties of as-grown  $\text{LiV}_2\text{O}_4$  (Sample A) and Li-ion intercalated  $\text{Li}_{1+x}\text{V}_2\text{O}_4$  films [A-1 ( $-2$  V), A-2 ( $-4$  V), and A-3 ( $-4.5$  V)]. (a) Out-of-plane XRD profiles. Inset:  $\omega$ -scan rocking curve profiles of  $\text{LiV}_2\text{O}_4$  111 reflections. (b) The magnification around the  $\text{Li}_{1+x}\text{V}_2\text{O}_4$  111 reflections. The solid and dashed lines indicate peak positions of 111 reflections for each sample. (c)  $\rho$ - $T$  curves of as-grown  $\text{LiV}_2\text{O}_4$  (Sample A) and Li-ion intercalated  $\text{Li}_{1+x}\text{V}_2\text{O}_4$  films (A-1  $\sim$  3). (d) The linear  $T^2$  dependence of resistivity for Samples A-1 and A-2 below 2 K.

(C-3). This result indicates that the MIT is induced by Li-ion electrochemical reactions.

In order to investigate correlation between structural and electronic properties, we prepared a number of  $\text{Li}_{1+x}\text{V}_2\text{O}_4$  films with different  $x$ . Using the setup shown in Fig. 3(a), the films cut out from Sample A were electrochemically doped under various potentials in air. Then, their *ex situ* properties were immediately characterized. Fig. 4(a) shows the out-of-plane XRD profiles for Li-ion intercalated  $\text{Li}_{1+x}\text{V}_2\text{O}_4$  films (Samples A-1, -2, and -3), prepared by applying different negative potentials ( $-2$ ,  $-4$ , and  $-4.5$  V, respectively), in a comparison with those for the pristine film. Neither the formation of secondary phases nor the degradation of crystallinity was observed. The  $\omega$ -scan rocking curve profiles were identical to each other [See inset of Fig. 4(a)]. These results suggest that the observed MIT was induced not by disorder but by electron doping associated with Li-ion

intercalation. Furthermore, systematic peak shift of the  $\text{LiV}_2\text{O}_4$  111 reflection was observed as magnified in Fig. 4(b). This inspection verifies the ideal topochemical reaction that excess Li ions distribute homogeneously over the samples while a host spinel lattice is maintained. According to the previous study for Li-ion intercalated polycrystalline  $\text{Li}_{1+x}\text{V}_2\text{O}_4$ , there is positive correlation between the amount of excess Li ( $x$ ) and the lattice constant [30]. Taking this relationship into account,  $x$  in Samples A-1, A-2, and A-3 were estimated to be 0.4, 0.5, and 1.2, respectively. Further details about the  $x$  dependence of lattice constant will be described later.

We noticed that peak shift between Samples A-2 ( $x \sim 0.5$ ) and A-3 ( $x \sim 1.2$ ) was substantially large [Fig. 4(b)]. Actually, two phases have been observed in the XRD profile of Samples A-4 ( $x \sim 0.8$ ) measured several days after applying  $-5$  V (see Fig. S1 in the Supplemental Material [31]). Interestingly, the peak position of one phase coincided with that of Samples A-3. Another one was located at slightly lower angle than Samples A-2, which corresponded to  $x \sim 0.6$ . Therefore, two phases coexist in a region of  $0.5 < x < 1$ .

Figure 4(c) shows the evolution of  $\rho$ - $T$  curves induced by systematic Li-ion intercalations. The  $\rho$  increased monotonically with increasing  $x$ , while apparent curve shapes of metallic samples remained intact. As for Sample A-3 with  $x \sim 1.2$ , insulating behavior was observed and HF behavior was no longer present. Taking this fact into account, the observed two structural phases are inevitably associated with metallic and insulating phases, respectively. The linear  $T^2$  dependence of  $\rho$  was obtained below 2 K for Samples A-1 and A-2, and  $A$  values were estimated to be  $9.6$  and  $18 \mu\Omega \text{ cm K}^{-2}$ , respectively [Fig. 4(d)]. Interestingly, Kondo-like upturns in  $\rho$  appeared below 1 K and became much remarkable with increasing  $x$ . This observation implies some insights for the origin of HF state in  $\text{LiV}_2\text{O}_4$ .

Let us discuss the observed MIT induced by electrochemical Li-ion intercalation. The oxidation state of vanadium in the initial  $\text{LiV}_2\text{O}_4$  is  $\text{V}^{3.5+}$  ( $3d^{1.5}$ ). As we described already, the same amount of electrons as excess Li ions is introduced. Thus, electron filling in Li ion intercalated  $\text{Li}_{1+x}\text{V}_2\text{O}_4$  films is  $3d^{1.5+x/2}$ . In this study, the system remains metallic up to  $x \sim 0.5$  ( $3d^{1.75}$ ), while the electron filling approaching to  $x \sim 1$  ( $3d^2$ ) leads to insulating states. The spinel-type  $M^{2+}\text{V}_2\text{O}_4$  ( $M = \text{Mg, Zn}$ ) with  $\text{V}^{3+}$  ( $3d^2$ ) are Mott insulators, and they are inferred to become metals at  $y \sim 0.6$  in polycrystalline  $\text{Li}_{1-y}M_y\text{V}_2\text{O}_4$  ( $3d^{1.8}$ ) from temperature dependence of Seebeck coefficient [14,16]. It is also worth mentioning that a Mott transition takes place around  $y = 0.2$  ( $3d^{1.8}$ ) in the perovskite-type  $\text{La}_{1-y}\text{Sr}_y\text{VO}_3$  [32]. On the basis of the similarity, the observed MIT in  $\text{Li}_{1+x}\text{V}_2\text{O}_4$  can be regarded as the Mott transition as approaching to  $3d^{1.8}$  ( $x \sim 0.6$ ). However, the critical filling parameter is not necessarily identical between different compounds and this intriguing correspondence needs further refinement. In addition to this issue, our results of transport measurements provide insight for HF behaviors in the vicinity of the Mott transition. Metallic conductivity with HF behaviors was robust as the system approaches to the metal-insulator phase boundary [Figs. 3(c) and 4(c)], which is in contrast to temperature dependence of resistivity seen for Sample B exhibiting metallic behavior around RT yet large upturn at low temperatures (Fig. 2).

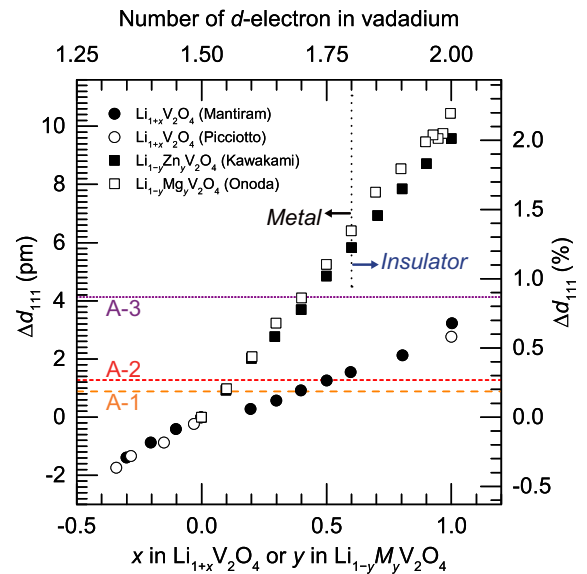


FIG. 5. Relationships between variations of lattice spacing  $\Delta d_{111}$  and contents of A cations in  $\text{Li}_{1+x}\text{V}_2\text{O}_4$  [20,30],  $\text{Li}_{1-y}\text{Zn}_y\text{V}_2\text{O}_4$  [14], and  $\text{Li}_{1-y}\text{Mg}_y\text{V}_2\text{O}_4$  [16]. The formal number of  $3d$  electrons in vanadium is indicated at the top abscissa.  $\text{Li}_{1-y}M_y\text{V}_2\text{O}_4$  ( $M = \text{Zn, Mg}$ ) systems are insulating in a region of  $y > 0.6$  ( $d^{1.8}$ ) (see text). The variation of  $\Delta d_{111}$  for the Li-ion intercalated films are shown by dashed lines.

The electrochemical Li-ion intercalation is a disparate approach enabling electron doping without introducing disorder [Fig. 4(a)]. This means that the adjustment of Li content by using PLD alone cannot prevent the formation of antisite defects (i.e.,  $\text{Li}[\text{Li}_x\text{V}_{2-x}]\text{O}_4$ ). Therefore, robust HF behaviors reflect the unique properties of  $\text{Li}_{1+x}[\text{V}_2]\text{O}_4$ , which have been so far hidden by the lack of sample quality (e.g., grain boundaries).

As we already mentioned, the previous study for Li-ion intercalated polycrystalline  $\text{Li}_{1+x}\text{V}_2\text{O}_4$  ( $-0.3 \leq x \leq 1$ ) revealed positive correlation between  $x$  and the lattice constant [30]. As seen in Fig. 4(b), systematic lattice expansion was also observed in Sample A. Figure 5 shows a comparison on the variation of lattice spacing  $\Delta d_{111}$  as a function of the formal number of  $3d$  electrons between bulks and our samples. We estimated  $x$  in Samples A-1 and A-2 to be 0.4 and 0.5, respectively, from the coincidence of  $\Delta d_{111}$  with those of polycrystalline  $\text{Li}_{1+x}\text{V}_2\text{O}_4$ . As for Sample A-3, the bulk dependence was extrapolated linearly to estimate  $x \sim 1.2$ . We note that electrochemical Li-ion intercalation has led  $x$  to be as large as 1.5, although no structural data is available [21].

The substitutional doping studies for  $\text{Li}_{1-y}M_y\text{V}_2\text{O}_4$  ( $M = \text{Zn, Mg}$ ) systems provide us important information about the role of lattice expansions in electron-doping driven MITs. The  $\Delta d_{111}$  of these systems reaches  $\sim 1.3\%$  at the metal-insulator phase boundary [ $y \sim 0.6$  ( $d^{1.8}$ )]. As for  $\text{Li}_{1+x}\text{V}_2\text{O}_4$ ,  $\Delta d_{111}$  was only  $\sim 0.3\%$  at  $x \sim 0.6$  ( $d^{1.8}$ ). Therefore, the electrochemical Li-ion intercalation allows more effective electron doping with suppressing the structural disorder and/or strain.

Systematic evolutions in HF behaviors and structural transitions are summarized in Fig. 6, where coefficient  $A$  and  $\rho$  at 2 K ( $\rho_{2K}$ ) are plotted against the amount of excess Li ( $x$ ). With increasing  $x$ , (i.e., number of  $3d$  electrons in vanadium),

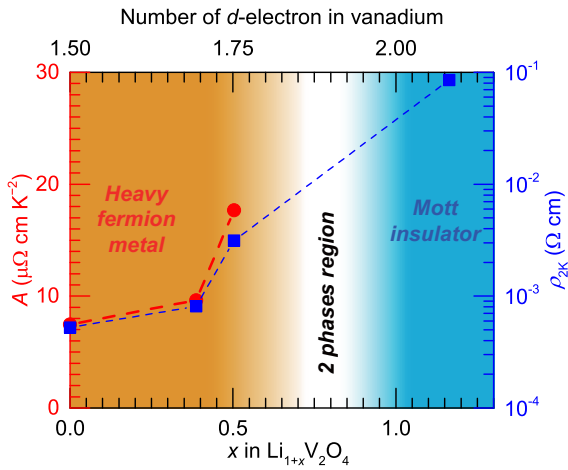


FIG. 6.  $A$  (left, circles) and  $\rho_{2K}$  (right, squares) as a function of  $x$  for  $\text{Li}_{1+x}\text{V}_2\text{O}_4$  films and number of  $d$  electrons in vanadium. Dashed lines are guides to the eye.

both quantities increase monotonically. Although an abrupt increase in  $A$  in the vicinity of the Mott transition is generally found [33], successive enhancement of  $A$  realized in  $\text{Li}_{1+x}\text{V}_2\text{O}_4$  implies exceptionally strong correlation. In fact,  $A$  reached  $18 \mu\Omega \text{ cm K}^{-2}$ , almost an order of magnitude larger than that of bulk.

Our study sheds light on the origin of HF state in  $\text{LiV}_2\text{O}_4$ , which has been ascribed to mixed-valent  $\text{V}^{3.5+}$  and/or geometrical spin frustration. According to the previous study,  $\text{LiV}_2\text{O}_4$  readily becomes a charge-ordered insulator below 20 K under moderate pressure of  $\sim 6.6$  GPa [11]. Conversely, it is believed that the mixed-valent  $\text{V}^{3.5+}$  state should play an important role in the formation of HF metallic state. Figure 6 demonstrates that such a condition is not necessarily specific to HF behaviors. We believe that geometrical spin frustration in triangular lattice is rather essential to HF behaviors in  $\text{Li}_{1+x}\text{V}_2\text{O}_4$ , as is often suggested in the previous studies [4,6,10]. In addition, the mechanism of insulating behavior observed in this study

is considered to be different from that of the pressure-induced one because of the opposite lattice deformation.

Apart from the fundamental point of view, our findings provide an interesting possibility. Thanks to mature technology for metal-oxide epitaxy, the fabrication of multilayer structures based on  $\text{LiV}_2\text{O}_4$  will not be a big challenge. In particular, such efforts are meaningful as artificial superlattices with the HF system of  $\text{CeIn}_3/\text{LaIn}_3$  have been recently demonstrated [34]. The extended study will harvest not only deep understanding of HF behaviors in  $\text{LiV}_2\text{O}_4$ , but also a novel opportunity to explore exotic properties of HF systems, for example, strongly coupled superconductivity in the two-dimensional HF system [35].

#### IV. SUMMARY

In summary, we have investigated the epitaxial growth of spinel-type  $\text{LiV}_2\text{O}_4$  films by PLD method and the effect of excess electrons on the transport properties of electrochemically Li-ion intercalated  $\text{Li}_{1+x}\text{V}_2\text{O}_4$  films. After optimizing the growth condition, high-quality  $\text{LiV}_2\text{O}_4$  epitaxial films exhibiting clear HF metallic behaviors were obtained. An electrochemical cell was implemented for the ideal Li-ion intercalation reactions. The increase in excess electrons in  $\text{Li}_{1+x}\text{V}_2\text{O}_4$  led to the enhancement of the HF behavior. These results demonstrate exceptionally strong electron correlation in  $\text{Li}_{1+x}\text{V}_2\text{O}_4$  in the vicinity of the Mott transition.

#### ACKNOWLEDGMENTS

The authors thank Prof. H. Tanaka for his support with transport measurements with PPMS equipped with the He-3 option. This work was partly supported by MEXT Elements Strategy Initiative to Form Core Research Center (Grant No. JPMXP0112101001) and a Grant-in-Aid for Scientific Research (No. 19H02588, No. 19K03711, No. 20K15169, and No. 21H02026) from the Japan Society for the Promotion of Science Foundation. T.Y. is supported by Chemistry Personnel Cultivation Program (Japan Chemical Industry Association).

- [1] A. C. Jacko, J. O. Fjærestad, and B. J. Powell, *Nat. Phys.* **5**, 422 (2009).
- [2] S. Kondo, D. C. Johnston, C. A. Swenson, F. Borsa, A. V. Mahajan, L. L. Miller, T. Gu, A. I. Goldman, M. B. Maple, D. A. Gajewski, E. J. Freeman, N. R. Dilley, R. P. Dickey, J. Merrin, K. Kojima, G. M. Luke, Y. J. Uemura, O. Chmaissem, and J. D. Jorgensen, *Phys. Rev. Lett.* **78**, 3729 (1997).
- [3] O. Chmaissem, J. D. Jorgensen, S. Kondo, and D. C. Johnston, *Phys. Rev. Lett.* **79**, 4866 (1997).
- [4] S. Kondo, D. C. Johnston, and L. L. Miller, *Phys. Rev. B* **59**, 2609 (1999).
- [5] D. C. Johnston, C. A. Swenson, and S. Kondo, *Phys. Rev. B* **59**, 2627 (1999).
- [6] C. Urano, M. Nohara, S. Kondo, F. Sakai, H. Takagi, T. Shiraki, and T. Okubo, *Phys. Rev. Lett.* **85**, 1052 (2000).
- [7] Y. Matsushita, H. Ueda, and Y. Ueda, *Nat. Mater.* **4**, 845 (2005).
- [8] R. Arita, K. Held, A. V. Lukoyanov, and V. I. Anisimov, *Phys. Rev. Lett.* **98**, 166402 (2007).
- [9] S. Das, X. Zong, A. Niazi, A. Ellern, J. Q. Yan, and D. C. Johnston, *Phys. Rev. B* **76**, 054418 (2007).
- [10] V. Yushankhai, T. Takimoto, and P. Thalmeier, *Phys. Rev. B* **82**, 085112 (2010).
- [11] A. Irizawa, S. Suga, G. Isoyama, K. Shimai, K. Sato, K. Iizuka, T. Nanba, A. Higashiya, S. Niitaka, and H. Takagi, *Phys. Rev. B* **84**, 235116 (2011).
- [12] Y. Shimizu, H. Takeda, M. Tanaka, M. Itoh, S. Niitaka, and H. Takagi, *Nat. Commun.* **3**, 981 (2012).
- [13] H. Okabe, M. Hiraishi, A. Koda, K. M. Kojima, S. Takeshita, I. Yamauchi, Y. Matsushita, Y. Kuramoto, and R. Kadono, *Phys. Rev. B* **99**, 041113 (2019).
- [14] K. Kawakami, Y. Sakai, and N. Tsuda, *J. Phys. Soc. Jpn.* **55**, 3174 (1986).
- [15] Y. Nakajima, Y. Amamiya, K. Ohnishi, I. Terasaki, A. Maeda, and K. Uchinokura, *Physica C* **185–189**, 719 (1991).

- [16] M. Onoda, H. Imai, Y. Amako, and H. Nagasawa, *Phys. Rev. B* **56**, 3760 (1997).
- [17] K. Yoshimatsu, M. Niwa, H. Mashiko, T. Oshima, and A. Ohtomo, *Sci. Rep.* **5**, 16325 (2015).
- [18] K. Yoshimatsu, T. Soma, and A. Ohtomo, *Appl. Phys. Express* **9**, 075802 (2016).
- [19] E. J. Fuller, F. E. Gabaly, F. Léonard, S. Agarwal, S. J. Plimpton, R. B. Jacobs-Gedrim, C. D. James, M. J. Marinella, and A. A. Talin, *Adv. Mater.* **29**, 1604310 (2017).
- [20] L. A. de Picciotto and M. M. Thackeray, *Mat. Res. Bull.* **20**, 1409 (1985).
- [21] G. Pistoia, M. Pasquali, L. A. de Picciotto, and M. M. Thackeray, *Solid State Ion.* **28**, 879 (1988).
- [22] L. A. de Picciotto, M. M. Thackeray, and G. Pistoia, *Solid State Ion.* **28–30**, 1364 (1988).
- [23] M. M. Thackeray, *J. Am. Ceram. Soc.* **82**, 3347 (1999).
- [24] S. Hamada, M. Kato, T. Noji, and Y. Koike, *Physica C* **470**, S766 (2010).
- [25] F. Simmen, T. Lippert, P. Novák, B. Neuenschwander, M. Döbeli, M. Mallepell, and A. Wokaun, *Appl. Phys. A* **93**, 711 (2008).
- [26] T. Tsuruhama, T. Hitosugi, H. Oki, Y. Hirose, and T. Hasegawa, *Appl. Phys. Express* **2**, 085502 (2009).
- [27] X. G. Qiu, C. Z. Bi, J. Y. Ma, X. Fang, M. Kamran, and B. R. Zhao, *Physica C* **460–462**, 540 (2007).
- [28] M. R. Harrison, P. P. Edwards, and J. B. Goodenough, *Philos. Mag. B* **52**, 679 (1985).
- [29] R. D. Shannon, *Acta Cryst. A* **32**, 751 (1976).
- [30] A. Manthiram and J. B. Goodenough, *Can. J. Phys.* **65**, 1309 (1987).
- [31] See Supplemental Material at <http://link.aps.org/supplemental/10.1103/PhysRevB.104.245104> for the out-of-plane XRD profiles providing the evidence for a two-phase region of  $0.5 < x < 1$ .
- [32] A. V. Mahajan, D. C. Johnston, D. R. Torgeson, and F. Borsa, *Phys. Rev. B* **46**, 10973 (1992).
- [33] Y. Tokura, Y. Taguchi, Y. Okada, Y. Fujishima, T. Arima, K. Kumagai, and Y. Iye, *Phys. Rev. Lett.* **70**, 2126 (1993).
- [34] H. Shishido, T. Shibauchi, K. Yasu, T. Kato, H. Kontani, T. Terashima, and Y. Matsuda, *Science* **327**, 980 (2010).
- [35] Y. Mizukami, H. Shishido, T. Shibauchi, M. Shimozawa, S. Yasumoto, D. Watanabe, M. Yamashita, H. Ikeda, T. Terashima, H. Kontani, and Y. Matsuda, *Nat. Phys.* **7**, 849 (2011).